Temporal characteristics of MHD modes initiating disruptions

V. Klevarova[1], P.C. de Vries[2], M. Lehnen[2], G. Pautasso[3], T. Markovic[4,5], M. Komm[4], J. Havlicek[4], J.A. Snipes[2], H. Zohm[3], G. Verdoolaege[1,6], JET contributors*, the EUROfusion MST1 team[+] and the ASDEX Upgrade team

[1] *Department of Applied Physics, Ghent University, Sint-Pietersnieuwstraat 41, B-9000 Ghent, Belgium*
[2] *ITER Organization, Route de Vinon sur Verdon, CS 90 046, 13067 St Paul Lez Durance, Cedex, France*
[3] *Max-Planck-Institut für Plasmaphysik, 85748 Garching, Germany*
[4] *Institute of Plasma Physics of the CAS, Za Slovankou 1782/3, 182 00, Prague, Czech Republic*
[5] *Faculty of Mathematics and Physics, Charles University, Prague, Czech Republic*
[6] *Laboratory for Plasma Physics, Royal Military Academy (LPP-ERM/KMS), B-1000 Brussels, Belgium*

1. Introduction

Tokamak disruptions represent a risk to large size devices (e.g. ITER) in terms of forces and heat loads deposited on the plasma facing components. The control system of such devices must thus embed a system for disruption prediction (with sufficient warning time) that will trigger mitigation actions if disruption avoidance fails [1]. Disruptions can be predicted by monitoring the growth of magnetohydrodynamic (MHD) instabilities that are eventually responsible for the loss of plasma confinement. MHD modes are observed to be locked (ML) or rotating (ROT) at the onset of the disruption. Furthermore, they are excited by various causes, motivating disruption classification. An empirical scaling law has been derived for the locked mode disruptive amplitude [2], allowing an estimate of the perturbation amplitude required to disrupt the plasma in ITER. However, the associated warning times, important for disruption prediction in ITER, have not yet been evaluated. Those might be determined by device geometrical parameters, plasma conditions and, potentially, by the disruption class and the associated type of MHD instabilities.

2. Multi-machine study of MHD mode endurance time

Fig.1 shows an example of an ASDEX Upgrade (AUG) discharge terminated by a disruption due to an initially rotating MHD mode. The perturbation locks at $t \sim 1.534\ s$, and the locked mode signal amplitude fluctuates before it grows monotonically and reaches the experimental disruptive amplitude, $B_{ML,disr}$, at the disruption onset, t_{disr}. Time-to-disruption (TtD) is defined as the time between the onset of a particular experimental level of $B_{ML,disr}$ and the t_{disr}, $t_{disr} - t_{ML,X\%\ level\ onset}$ (e.g., 50% TtD interval II. in *Fig.1*). Those temporal intervals carry information concerning the mode growth characteristics, e.g. the phase of the explosive amplitude growth. The total mode duration to the disruption onset is illustrated by the time interval I. in *Fig.1*. The major disruption time t_{disr} corresponds to the current quench onset (set to the onset of the last plasma current spike) and is depicted by a red vertical line in *Fig.1*.

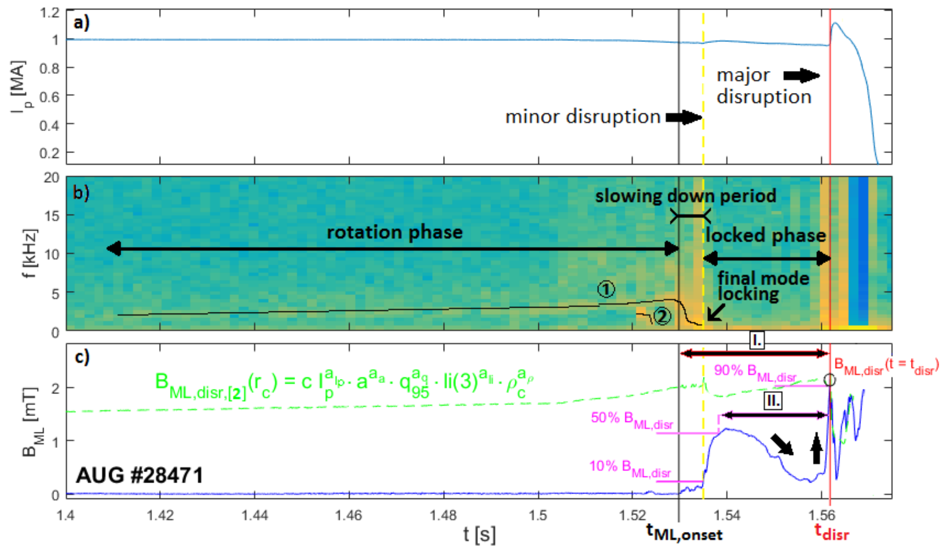

Fig.1. Example of an AUG disruptive discharge, caused by an initially rotating MHD mode ① observable from $t \sim 1.410\ s$ *on b) (mode ② was not studied). Locked mode amplitude surpasses noise level at* $t = t_{ML,onset}$. *At* $t = t_{disr}$ *the experimental mode amplitude approaches the scaled threshold [2], depicted by the green dashed line.*

To study a potential relationship between the mode temporal characteristics and the geometrical device parameters, a multi-machine database of disruptive discharges has been built. In all cases an MHD mode was the final disruption precursor. The database consists of 318 JET-ILW, 457 AUG full-W, and 37 COMPASS shots. TtD for 10, 50 and 90% of the experimental disruptive amplitude have been determined for each entry in the database, together with the mode duration. TtD for the three experimental levels and devices are plotted vs. the normalized accumulated fraction of disruptions (FD) in *Fig.2a)*. Time scales associated with the mode duration are spread over 2, 4 and 5 orders of magnitude in case of COMPASS, AUG and JET, respectively, suggesting a complex interplay of variables determining the mode duration. The longest mode durations in JET and AUG are of the order of the resistive diffusion time scale, $\tau_{res} = \mu_0 \sigma a^2$, a being the plasma minor radius. Assuming the same plasma conductivity σ for JET and AUG ($T_{e,JET} \approx T_{e,AUG}$), $a_{JET}/a_{AUG} \sim 2$, therefore $\tau_{res,JET}/\tau_{res,AUG} \sim 4$ which is a factor recognisable in the tail of the two $\{t_{disr} - t_{ML\ onset}\}$ curves ($\sim 0.5\ s$ and $\sim 2\ s$ for AUG and JET, respectively). The shortest time scales, on the other hand, might be influenced by the data time sampling, sensor specifications etc. For a given FD = 50%, the TtD for 10, 50 and 90% of $B_{ML,disr}$ is plotted as a function of device minor radius a in *Fig.2b)*. The data points seem to follow a monotonic trend line, as do the medians of the mode durations. However, results from analogical study in DIII-D [3] might not confirm the trend. More devices will be thus added to the database and the underlying physics will be examined.

The difference in the shape of the 90% TtD curves of AUG and JET might be due to the fact that the majority of AUG disruptions are caused by the density limit (section 3), for which gradually growing modes are typical, while in JET case most of the disruptions are due to the accumulation of high-Z material in the plasma core [4], where the modes grow explosively at the early stage of the locked phase.

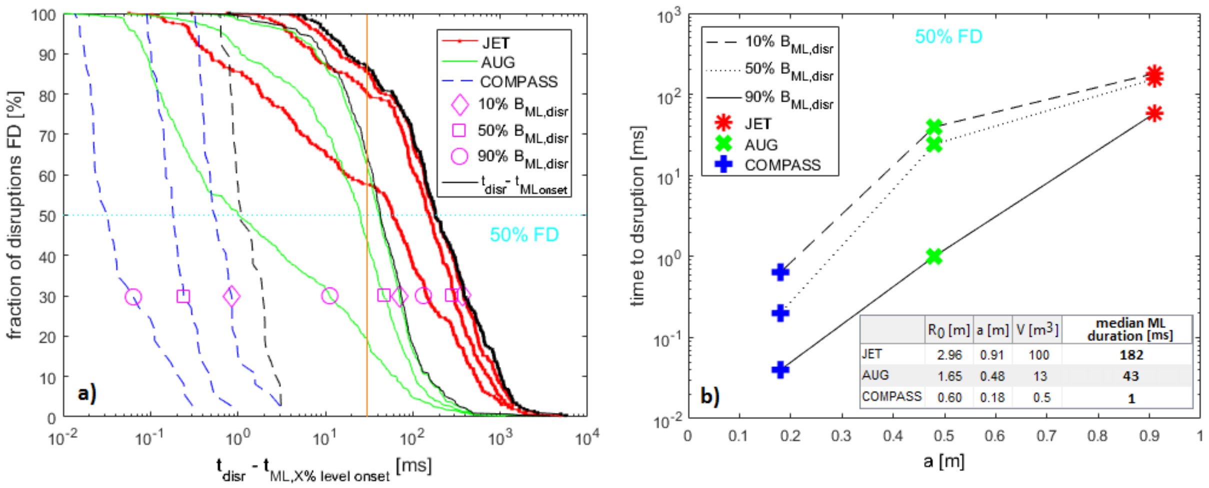

Fig.2,a) The FD vs. 10, 50 and 90% TtD for three devices (JET, AUG, COMPASS). In black are displayed $t_{disr} - t_{ML\ onset}$ time intervals. Disruptions caused by rotating modes are discarded from the plot. The orange vertical line depicts the minimum warning time for ITER disruption mitigation (30 ms). b) The 10, 50 and 90% TtD plotted as a function of the device minor radii taken at 50% FD.

3. Dependence of the locked mode duration on disruption class (AUG)

In the context of disruption prediction based on threshold mode amplitude, it is of interest to determine whether the mode enters the disruptive process within a warning time interval that allows for triggering disruption mitigation. This time interval can be class-dependent. AUG database entries were thus classified into 8 disruption groups (*Figure 3*, table). About 50% of AUG database entries fell into the density limit category. Graphically it is possible to distinguish different time scales related to distinct disruption classes on the $\{t_{disr} - t_{ML,X\%\ level\ onset}\}$ curves in *Fig.3*. Fast growing and short lasting modes seem to accompany disruptions due to radiative collapse, while on the opposite part of the spectra are error field locked modes and neoclassical tearing modes. The rest of the classes appear to be evenly distributed.

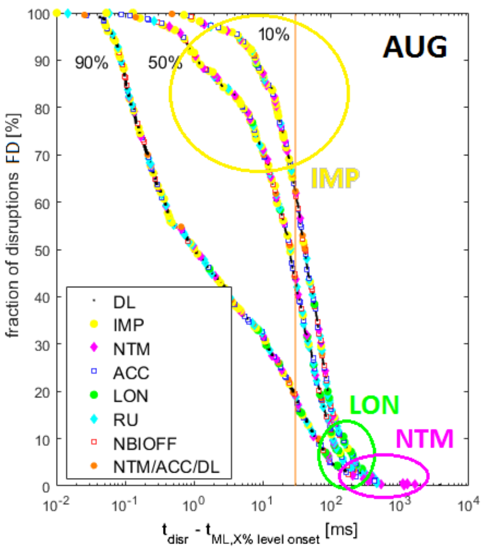

class code		relative occurrence [%]	median ML endurance time [ms]
DL	density limit	50	45
IMP	high impurity content->radiative collapse	11	11
NTM	neoclassical tearing mode	7	26
ACC	in-core high-Z material accumulation	12	27
LON	error field locked modes	2	153
RU	disruptions during plasma ramp-up	9	92
NBIOFF	density limit following NBI switch off	6	62
NTM/ACC/DL	combination of above	3	28

Fig.3. The FD vs. 10, 50 and 90% TtD (AUG). The disruptive class for each entry in the database is depicted by the corresponding marker. Note the three regions predominantly populated by one particular class. Table: Explanation of class coding, relative occurrence of the particular disruption cause in database and medians of mode durations.

4. Rotating MHD precursors initiating disruptions (JET)

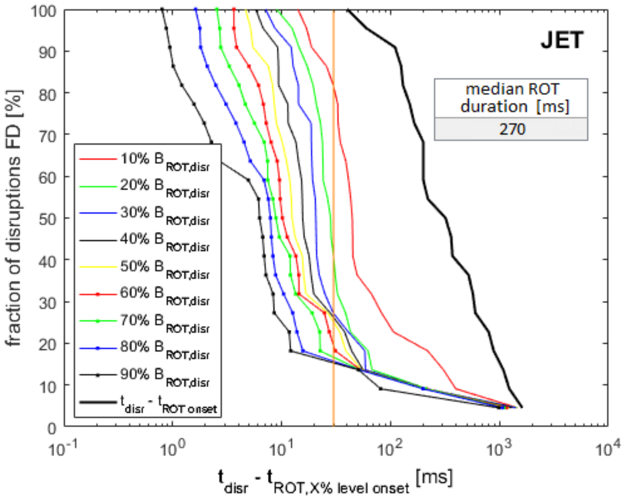

Fig.4. The FD vs. 10-90% TtD for 22 JET disruptions caused by a rotating mode.

In ~ 5% and ~ 8% of AUG and JET disruptive shots, respectively, the major disruption was caused by a rotating mode. This represents a percentage of disruptions that could not be predicted when relying solely on locked mode sensors. The amplitudes of rotating modes causing disruptions in 22 JET discharges were retrieved and 10-90% TtD vs. FD is shown, together with the total mode durations, in *Fig.4*. The latter exceeds 40 ms in all cases, compared to 83% FD in the case of locked modes (*Fig.2*). On the other hand, a significant growth of mode amplitude is typically observed just a few tens of milliseconds before the disruption, which is graphically readable as a significant temporal gap between the $\{t_{disr} - t_{ROT,10\%\ level\ onset}\}$ and $\{t_{disr} - t_{ROT\ onset}\}$ curves in *Fig.4*.

5. Summary

In the context of disruption prediction, it is important to determine parameters influencing the mode duration. According to the results presented here, those could be device and disruption-class dependent. A multi-machine comparative approach is important to provide a reliable scaling of locked mode amplitude-based warning times for disruption prediction in ITER.

Experimental data from AUG and JET show that 100% success rate in those devices would not be met with only locked mode amplitude used for disruption prediction. Developing reliable multi-parameter disruption prediction algorithms may be necessary to achieve the success rate requirements in ITER (eventually > 95%). The amplitude of rotating modes may be a good candidate signal in this context and it is important to examine what determines the fraction of rotating modes triggering disruptions.

[1] M. Lehnen et al., "*Control, detection and mitigation of disruptions on ITER*", 2015 IEEE 26th SOFE, 2015
[2] P.C. de Vries et al., Nucl. Fusion 56 (2016) 56026007
[3] R. Sweeney et al., Nucl. Fusion 57 (2017) 016019
[4] P.C. de Vries et al., Nucl. Fusion 51 (2011) 053018

This work was supported by the European Commission, carried out within the frameworks of the Erasmus Mundus International Doctoral College in Fusion Science and Engineering (FUSION-DC) and of the EUROfusion Consortium and has received funding from the Euratom research and training programme 2014-2018 under grant agreement No 633053. The views and opinions expressed herein do not necessarily reflect those of the ITER Organization or the European Commission.

** X. Litaudon et al., Overview of the JET results in support to ITER, accepted for publication in Nuclear Fusion*

+ H. Meyer et al., Overview of progress in European Medium Sized Tokamaks towards an integrated plasma-edge/wall solution, accepted for publication in Nuclear Fusion